catalysts

Supporting Information

Constructing active sites on self-supporting $Ti_3C_2T_X$ (T = OH) nanosheets for enhanced photocatalytic CO_2 reduction into alcohols

Shuqu Zhang, Man Zhang, Wuwan Xiong, Jianfei Long, Yong Xu, Lixia Yang, Weili Dai*

Key Laboratory of Jiangxi Province for Persistent Pollutants Control and Resources Recycle, Nanchang Hangkong University, Nanchang 330063, Jiangxi Province, People's Republic of China

*** Corresponding author:**

Email: wldai81@126.com, daiweili@nchu.edu.cn (W. Dai)

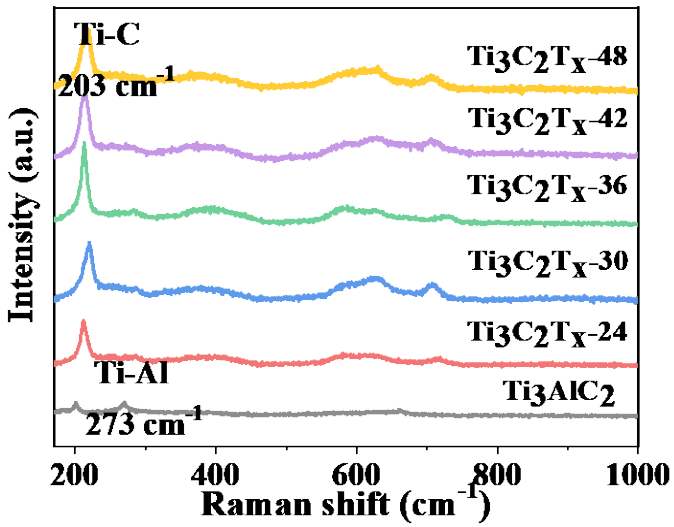

Figure S1. Raman spectra of Ti_3AlC_2, $Ti_3C_2T_x$-y nanosheets (y= 24, 30, 36, 42 and 48).

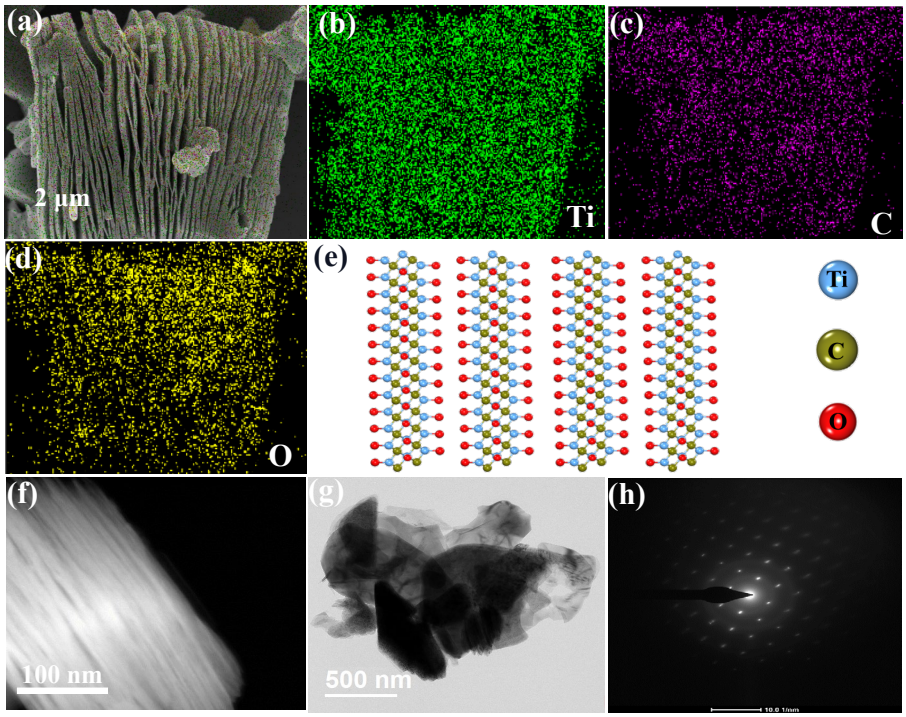

Figure S2. SEM image of (a) $Ti_3C_2T_x$-36, (b-d) elemental mappings of (a). (e) Atomic structure of $Ti_3C_2T_x$, (f) STEM image, (g) TEM image and (h) selected area electron diffraction (SAED) pattern of $Ti_3C_2T_x$-36.

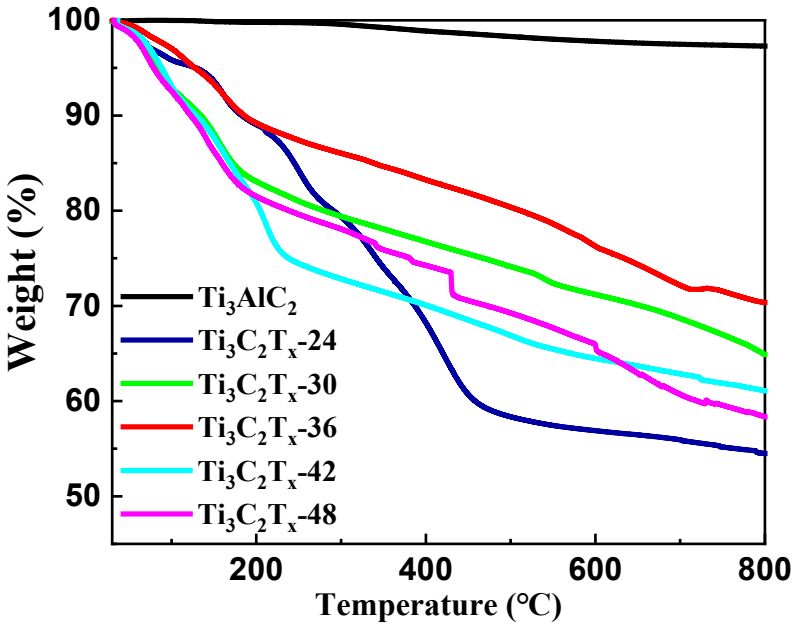

Figure S3. TG analysis of (a) Ti_3AlC_2, (b) Ti_3C_2Tx-24, (c) Ti_3C_2Tx-30, (d) Ti_3C_2Tx-36, (e) Ti_3C_2Tx-42 and (f) Ti_3C_2Tx-48.

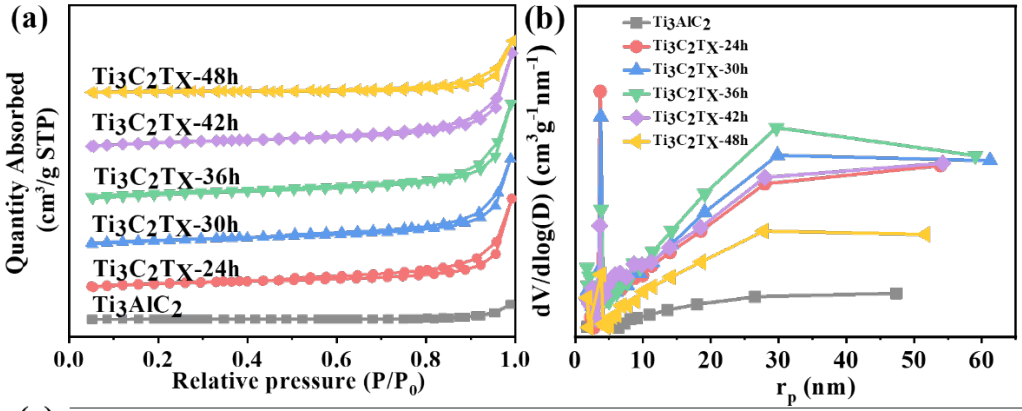

(c)

Samples	BET surface area (m^2/g)	Pore size (nm)	Pore volume (cm^3/g)
Ti_3AlC_2	0.56	17.33	0.0022
$Ti_3C_2T_X$-24	2.49	17.33	0.0127
$Ti_3C_2T_X$-30	3.27	15.23	0.0125
$Ti_3C_2T_X$-36	3.52	15.62	0.0138
$Ti_3C_2T_X$-42	2.97	16.93	0.0135
$Ti_3C_2T_X$-48	1.41	21.36	0.0076

Figure S4. (a) Nitrogen adsorption−desorption isotherms, (b) corresponding pore size distribution curves, and (c) information contrast of BET surface area, pore size and pore volume of $Ti_3C_2T_X$ with different etching times.

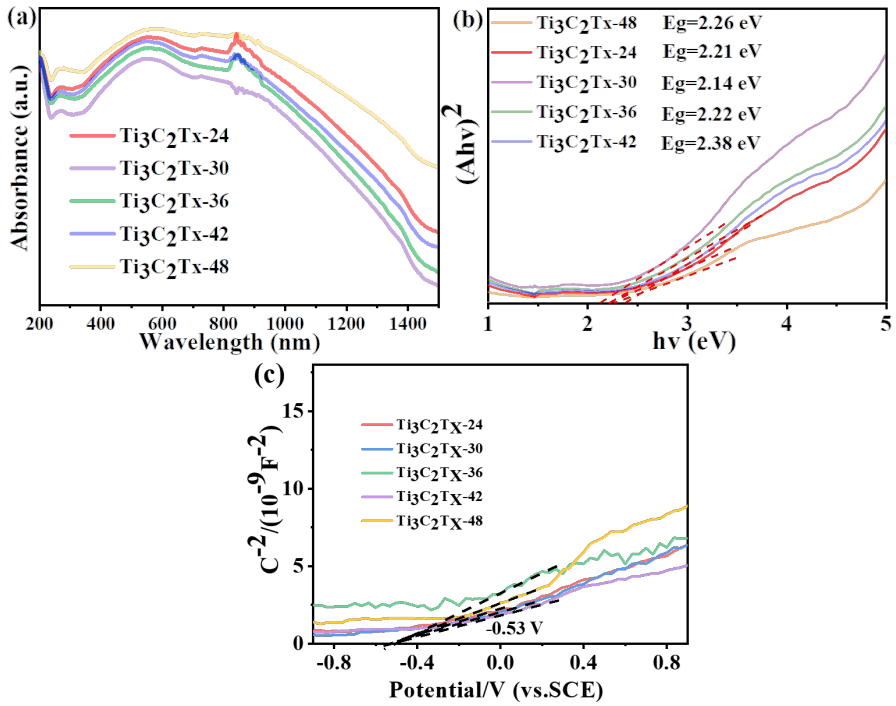

Figure S5. (a) UV-vis absorption spectra, (b) Plots of transformed Kubelka–Munk function $(Ahv)^2$ *vs* light energy (hv) and (c) Mott-Schottky spectra of Ti_3C_2Tx-24, Ti_3C_2Tx-30, Ti_3C_2Tx-36, Ti_3C_2Tx-42, Ti_3C_2Tx-48.

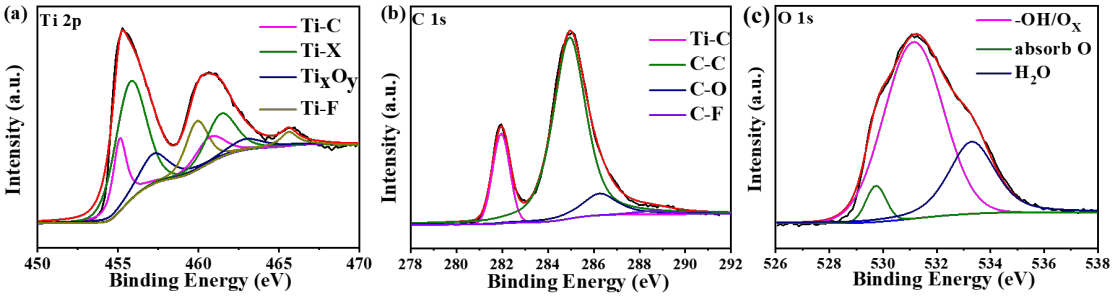

Figure S6. High-resolution XPS spectra of (a) Ti 2p, (b) C 1s and (c) O 1s over $Ti_3C_2T_x$-36.

Table S1. The comparison of photocatalytic activity for CO_2 reduction (products: methanol and ethanol) by some photocatalyst systems.

No.	Photocatalyst	Reaction conditions	Products	Formation rate ($\mu mol\ g^{-1}\ h^{-1}$)	Ref.
1	Au-ZIF 67	150 mW/cm^2 TEOA	CH_3OH C_2H_5OH	2500 500	27
2	Cu-TiO_2/GO	Hg lamp	CH_3OH C_2H_5OH	157 265	28
3	Cu /UiO-66-NH_2	300 W Xenon lamp λ>400 nm TEOA	CH_3OH C_2H_5OH	5.33 4.22	29
4	Pt/N-BiOCl	300 W Xenon lamp	CH_3OH C_2H_5OH	41.09 1.65	30
5	Co/g-C_3N_4	300 W Xenon lamp 1.5 W/cm^2	CH_3OH	235.48	31
6	Gd/BiOBr	300 W Xenon lamp λ>420 nm	CH_3OH	41.24	32
7	Bi_2WO_6	LED lamp	C_2H_5OH	68.9	33
8	TiO_2/rGO/CeO_2	Hg lamp	CH_3OH C_2H_5OH	641 271	34
9	Bi_2MoO_6	LED lamp 810 W/cm^2	C_2H_5OH	34.4	35
10	Cu/Pt-$HCa_2Ta_3O_{10}$	100 mW/cm^2	CH_3OH C_2H_5OH	113 7.4	36
11	$Ti_3C_2T_x$	300 W Xenon lamp λ>420 nm	CH_3OH C_2H_5OH	9.525 5.725	This work

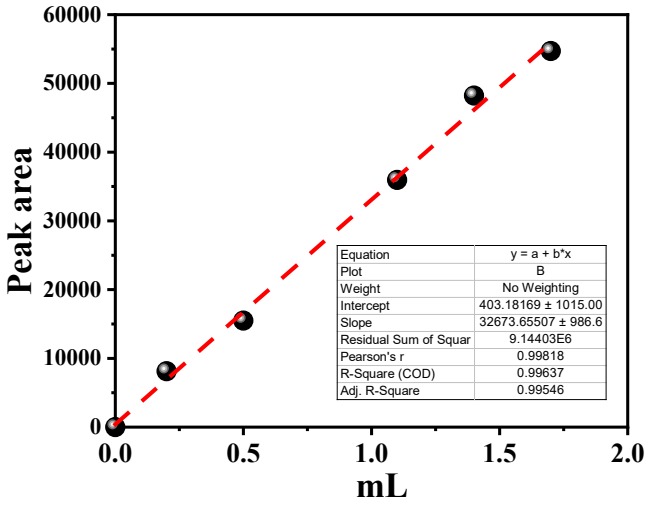

Figure S7. Calibration curves of the relationships between peak area and O_2 volume.

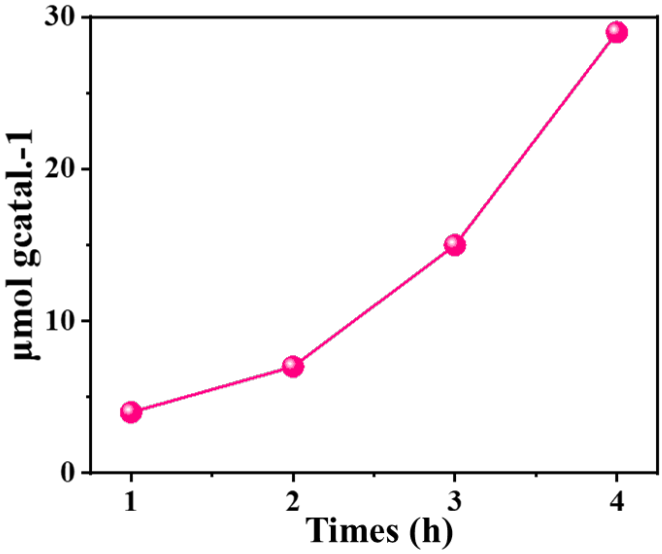

Figure S8. O_2 evolution during photocatalytic CO_2 reduction over $Ti_3C_2T_x$-36.